Indoor temperature variability in the Sahel: a pilot study in Ouagadougou, Burkina Faso.

Benjamin Pohl, Stéphanie dos Santos, Guy Martial Bai, Yacouba Compaoré, Kassoum Dianou, Julita Diallo-Dudek, Abdramane Soura, Serge Janicot

Indoor temperature variability in the Sahel: A pilot study in Ouagadougou, Burkina Faso

Benjamin Pohl[1]*, Stéphanie Dos Santos[2], Guy Martial Bai[3], Yacouba Compaoré[3,4], Kassoum Dianou[3], Julita Diallo-Dudek[1,5], Abdramane Soura[3], Serge Janicot[6]

[1] Centre de Recherches de Climatologie, UMR6282 Biogéosciences, CNRS / Univ. Bourgogne Franche-Comté, Dijon, France
[2] Laboratoire Population Environnement Développement, IRD/AMU, Université Félix Houphouët-Boigny, Cocody, Abidjan, Côte d'Ivoire
[3] Institut Supérieur des Sciences de la Population, Université Joseph Ki-Zerbo, Ouagadougou, Burkina Faso
[4] Centre de Recherche en Démographie (DEMO), Université Catholique de Louvain, Louvain la Neuve, Belgium
[5] Maison des Sciences de l'Homme – USR CNRS 3516 Université de Bourgogne, Dijon, France
[6] Laboratoire d'Océanographie et du Climat: Expérimentations et Approches Numériques, LOCEAN, Sorbonne Université (UPMC), IRD, CNRS, MNHN, Paris, France

Pohl B, S Dos Santos, GM Bai, Y Compaoré, K Dianou, J Dudek, A Soura & S Janicot (2021) Indoor temperature variability in the Sahel: A pilot study in Ouagadougou, Burkina Faso. Theoretical and Applied Climatology, 146, 1403-1420. doi:10.1007/s00704-021-03800-z

*** Corresponding Author's Address**
Laboratoire Population Environnement Développement
IRD/AMU, Université Félix Houphouët-Boigny
Cocody, Abidjan, Côte d'Ivoire
stephanie.dossantos@ird.fr

Abstract

Very little research has documented the exposure of populations in Africa to extreme heat. We measured indoor air temperature and humidity hourly for 13 months in seven houses of contrasted architecture and construction materials all in the northern neighbourhoods of Ouagadougou, Burkina Faso. These measurements are compared to air temperatures recorded at the synoptic weather station of Ouagadougou airport and to land surface temperature estimates from Landsat satellite images at seven dates with clear-sky conditions.

The results reveal huge temperature differences (exceeding 10 °C) between houses, especially in the afternoon hours of the warmest season. Indoor temperature is also much more variable than land surface (outdoor) temperature in the same locations, as estimated by satellite imagery. Houses with greater thermal inertia smooth the afternoon temperature peak, reducing heat exposure. Heat stress bioindicators reveal that danger thresholds, while rarely reached in some houses are frequently exceeded in others year round except for the core of the cold winter season (December and January). In spring, the hottest season, the danger threshold is almost permanently exceeded in these dwellings, exposing their inhabitants to significant heat stress.

This pilot study shows the primary role of housing in modulating indoor temperature, raising questions of public health and habitability of Sahelian regions in a warming world. This issue will be of increasing importance with ongoing climate change. Hence the need for further, more detailed instrumented campaigns in African settlements.

Key words

Indoor temperatures, climate change, heat stress, human well-being, Sahel, African housing

Highlights

1. Indoor temperatures vary tremendously between houses
2. Contrasts between houses are greatest in the hottest hours of the warm season
3. Thermal danger or extreme danger levels are often exceeded in some houses
4. In some houses, heat stress may occur in all seasons except winter
5. More instrumented campaigns for heat stress in African housing are needed

1. Introduction

The consequences of extreme temperatures on human well-being are now well documented in high-income countries, since different heat wave (HW) events have led to the premature death of thousands of people there (Gasparrini et al. 2015). But such issues are still to be addressed in low- and middle-income countries (hence among the most vulnerable: Ahmadalipour et al. 2019). This is particularly true of sub-Saharan Africa, which could bear the heaviest regional burden of climate change (Costello et al., 2009). The lack of data (fine-scale climate data, reliable and representative health data, and exhaustive mortality databases) partly explains our limited understanding of the society–health–climate inter-relationships in these regions. This gap is particularly striking for the densely-populated Sahelian region of West Africa. There, temperatures have soared since at least the mid-1970s, as a regional response to increasing greenhouse gas concentrations driven by anthropogenic activities (Lavaysse 2015; Moron et al. 2016). This warming, which is particularly marked during the hottest season, the northern-hemisphere spring (Oueslati et al. 2017), is even accelerating and is now clearly discernible not only in mean temperature, but also across a wide range of derived thermal indicators (Moron et al. 2016), including climate extremes like HWs (Ringard et al. 2016; Barbier et al. 2018; Sambou et al. 2020). The fifth Intergovernmental Panel on Climate Change assessment report (IPCC 2013) concluded that anthropogenic warming will continue in Africa throughout the twenty-first century, leading to HWs of increased frequency, duration and severity (Russo et al. 2014, 2016; Diedhiou et al. 2018; Sambou et al. 2021).

Very little research has been done to understand and characterize the vulnerability of populations to the increasing risks associated with exposure to extreme heat (Gough et al. 2019; Tyubee et al. 2020), especially in Africa. Major risk factors appear to include environmental living conditions such as the lack of air conditioning (Naughton et al. 2002; Semenza et al. 1996) or bathrooms (Larrieu et al. 2008), or the quality of thermal insulation, especially for rooftop apartments (Vandentorren et al. 2006). Recent studies have attempted to develop early warning systems for extreme events like HWs through seamless climate predictions and forecasts (e.g., Baso et al. 2019; Moron et al. 2019; Dirmeyer et al. 2020). Coupled with relevant indexes and criteria (Anderson et al. 2013), they can be used to anticipate high-impact events (Majumdar et al. 2020), including – but not restricted to – deadly heat (Matthews et al. 2017, 2019; Mora et al. 2019). Xu et al. (2016) identified three main criteria for heat exposure: the temperature itself (minimum, maximum, average temperature), and the intensity and length of time spent above a given (physiological) temperature threshold. Yet, in most cases, only the outdoor temperature is considered, thereby overlooking the heat stress and danger experienced by the body indoors.

Tham et al. (2020) highlight that high indoor temperatures affect several aspects of human health, in particular respiratory health, diabetes and mental health. For healthy children, temperature differences of 20 to 30 °C are linked to significant variations in cardiorespiratory disorders during sleep (Franco et al. 2000). One of the few studies in Africa involves 574 randomly sampled adults aged between 18 and 65 years from Ghana, and shows that a rise in ambient temperature is associated with a fall in blood pressure (Kunutsor and Powles 2010). Temperature data loggers were placed in classrooms in Yaoundé and Douala (Cameroon) and a survey of the pupils conducted. The results reveal an association between rising temperatures and a perception of discomfort such as headaches, fatigue, and extreme heat discomfort (Dapi et al. 2010). However, the temperature threshold at which adverse effects gradually begin has not been clearly identified, mostly due to lack of data (Tham et al. 2020). Hence the need to develop research in this field. The

latest World Health Organization Housing and Health Guidelines also called for more research on indoor temperatures, and in particular on the maximum temperatures above which health risks increase significantly (WHO, 2018). A major difficulty may be that indoor thermal conditions are expected to be highly dependent on the buildings' architecture and surroundings (Tyubee et al. 2020). As this issue is increasingly important because of ongoing climate change, a few recent studies have focused on indoor heat and thermal conditions in Nigeria (Adunola 2014), Tanzania (Von Seidlein et al. 2017) and South Africa (Adesina et al. 2020). Yet none of these studies considered Sahelian cities, in spite of the combination of various phenomena (intense climate warming and variability compounding existing hot climatic conditions, high population density, urbanization under demographic growth) that could cause, rapidly and recurrently, severe public health issues and major heat danger.

The present paper aims at filling this gap. It presents the results of a pilot study in Ouagadougou, the capital and largest city of Burkina Faso, that consisted in measuring indoor temperature in different types of housing and in different residential areas. The instrumented campaign lasted about 13 months (April 2017 to May 2018) and involved seven houses with contrasted construction materials and architectures. Here, we document how indoor temperatures vary in time and between houses, even in the same neighbourhood. We also study the relationship between indoor and outdoor temperatures, and attempt to separate the respective influences of outdoor climate and building characteristics. House responses to rapid temperature changes are also assessed to analyse their thermal inertia, and associated consequences for inner heat comfort. To that end, bioclimatic indices combining air temperature and humidity are used to estimate the heat stress experienced by the human body in these houses.

Section 2 presents the data and methods used in this study (including a description of the seven houses). Section 3 presents the main results obtained during the instrumented campaign. Section 4 summarizes the main results and Section 5 discusses their implications.

2. Data and Methods

2.1 The Ouagadougou – Health and Demographic Surveillance System (Ouaga-HDSS)

The study was conducted between 25 April 2017 and 22 May 2018 in the Ouagadougou – Health and Demographic Surveillance System (Ouaga-HDSS: Rossier et al. 2012) field site (Fig. 1). One of the objectives of this multidisciplinary project is to measure the impact of HWs on human health for households residing in the neighbourhoods concerned. In 2018, the population of these five neighbourhoods was estimated at almost 100,000, half of whom are largely illiterate and live in very rudimentary economic conditions and housing in informal areas (Dos Santos 2019). In this sector, seven houses were selected to monitor indoor temperature and humidity hourly (giving a total of 9432 measurements for each house over the study period). Some missing values are due to maintenance or early removal of data loggers at the inhabitants' request. From these variables, we computed hourly heat index (HI) values, following the formula of Steadman (1979) modified by the U.S National Weather Service. HI is a nonlinear function of temperature (T) and relative humidity (RH) that determines the human-perceived equivalent temperature. High RH limits human thermoregulation by evaporative cooling and so amplifies the heat stress of temperature extremes. Climatic conditions become dangerous for human health (high risk of heat stroke and

muscle cramps) for a HI above 40 °C and extremely dangerous for HI values exceeding 52–54 °C (Steadman 1979).

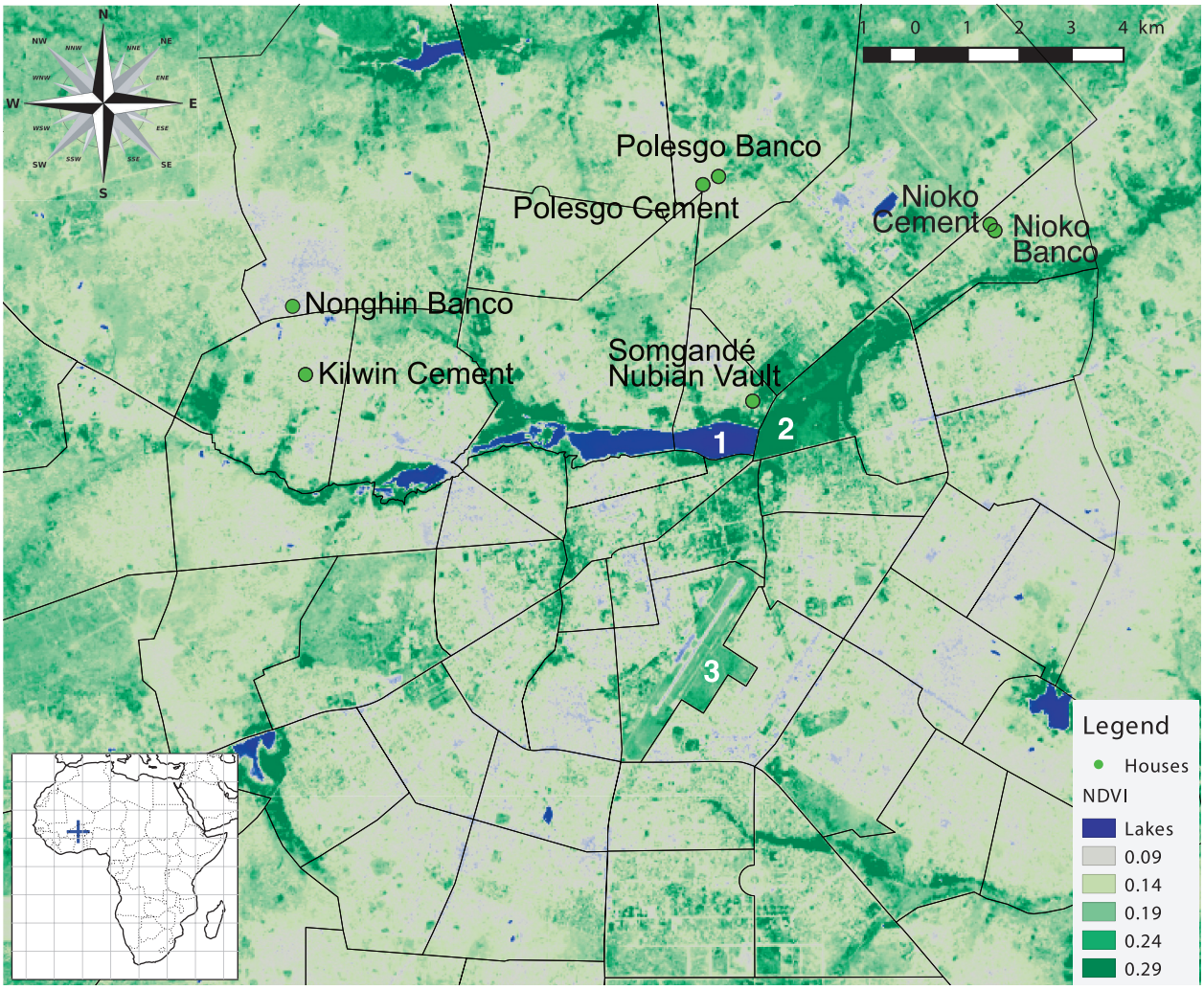

Figure 1 General map of Ouagadougou, Burkina Faso. Colours show vegetation activity (Normalized Difference Vegetation Index) estimated from Landsat imagery on 25 December 2017. The green dots mark the location of the seven houses under study. Numbers are for: (1) water reservoirs; (2) Bangr Weogo park (forested land); (3) the international airport.

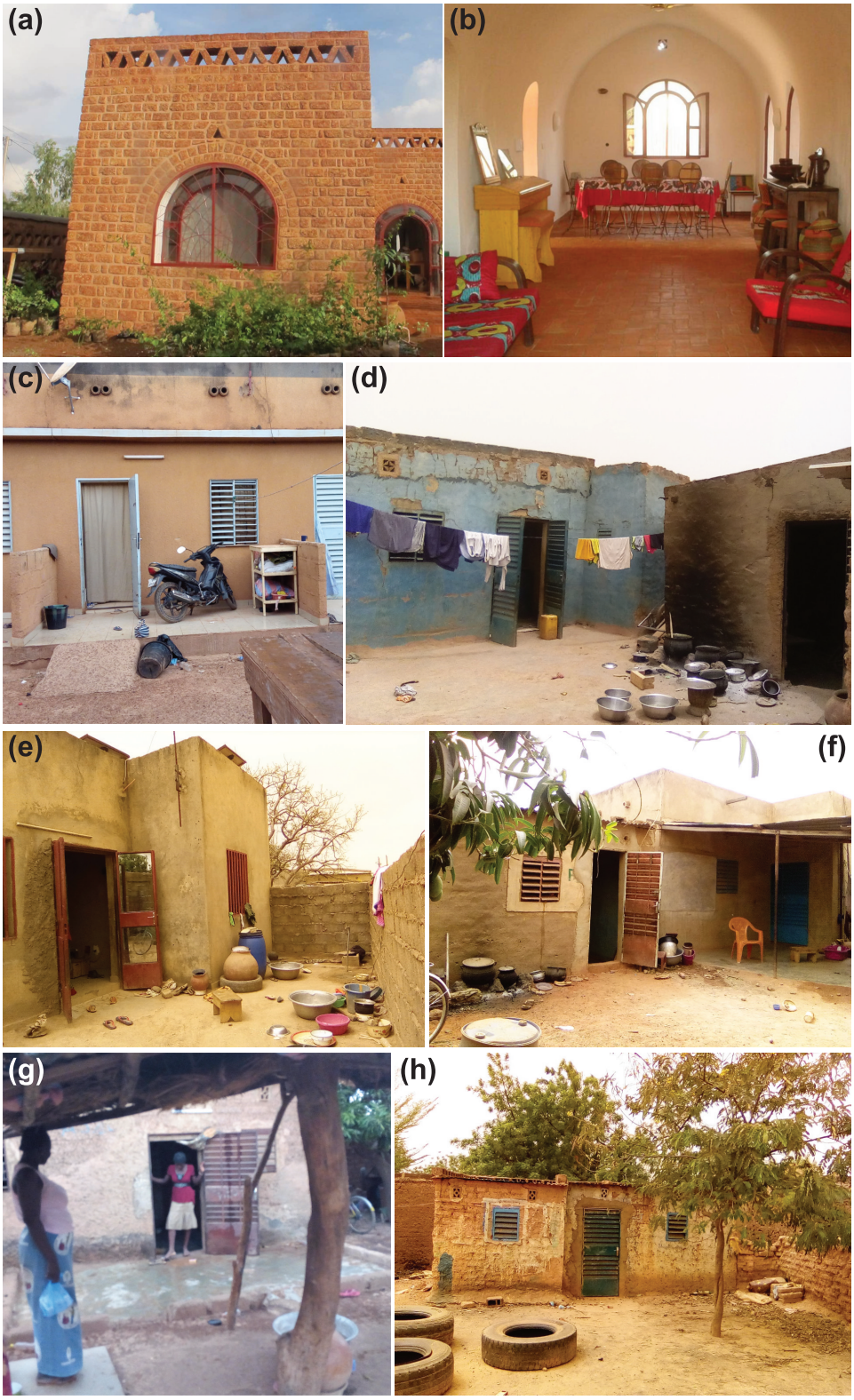

Figure 2 Pictures of the seven houses. (a–b) Somgandé Nubian Vault; (c) Kilwin Cement; (d) Nonghin Banco; (e) Nioko Cement; (f) Nioko Banco; (g) Polesgo Cement; (h) Polesgo Banco. See main text and Table 1 for details.

	Flooring material	Roofing material	External wall material	Room area	Room usage
Kilwin Cement	Ceramic tiling	Sheet metal on concrete slab	Cement	11 m^2	Bedroom
Nioko Banco	Cement	Sheet metal	Improved mud	10 m^2	Bedroom
Nioko Cement	Ceramic tiling	Sheet metal	Cement	20 m^2	Living room
Nonghin Banco	Cement	Sheet metal	Improved mud	10 m^2	Bedroom
Polesgo Cement	Cement	Sheet metal	Improved mud	12 m^2	Living room
Polesgo Banco	Cement	Sheet metal	Simple mud	13 m^2	Bedroom
Somgandé Nubian Vault	Clay tiling	Earth	Much improved mud	30 m^2	Living room

Table 1 Presentation of the seven houses and their characteristics.

Houses were selected depending on the household's willingness to accept the presence of a data logger, which was a major difficulty in this work. The population was generally very reluctant to participate in this pilot survey. It took a lot of patience from the investigators to find households willing to allow the devices to be fitted and a lot of explanations about the guarantees as to privacy. This point was crucial because the data loggers were placed in the bedroom to monitor the thermal conditions experienced by the human body indoors. The choice of the houses was also made to include diversity in the environmental living conditions of the households. The objective was therefore to diversify, in all five neighbourhoods, the types of housing, walls, and roofing. This diversity also reflects the range of lifestyles and socio-economic characteristics observed there (Table 1; Fig. 2).

- In the neighbourhood of Kilwin, the "Kilwin Cement" dwelling is located in a "celibatorium", a single-storey set of three dwellings with a shared courtyard. The house comprises a living room and a bedroom (with a bathroom in the bedroom). The roof is made of sheet metal on a concrete slab, the floor is tiled and the external walls are made of cement. The bedroom, where the data logger was placed, has a louvre window with iron nako (that is, window frames allowing the movement of metal or glass slats about twenty centimetres wide, like shutters), in front of the entrance door of the room, ideal for natural ventilation. During the period, a ceiling fan was installed above the bed where three people sleep (a couple and their young child). The data logger was placed on the wall between the bedroom and the living room, with no direct exposure to sunlight. Outside, the shared courtyard and the building are fully exposed, with no shading effect.
- The house of "Nonghin Banco" is composed of three rooms where five people (two adults and three children) live. With a simple sheet metal roof, cement floor, and outer walls made

of improved banco (a traditional building material in sub-Saharan Africa, made of clay and chopped straw), it is located in a densely populated informal neighbourhood. The room where the data logger was placed is one of two bedrooms with a small and a large louvre window made of iron nako. The wall to which the data logger was fitted is south-facing, just in front of another building less than 1 metre away, providing shade in the afternoon. The courtyard is not shaded at all, despite the presence of a young tree (less than 1 m high at the time the logger was installed). The wife of the head of the household sells take-away lunches made on stoves in the courtyard, not far from the wall of the monitored room. The parents said they sleep outside during the hot season because the indoor temperature is too high. For safety reasons, the children sleep indoors.

- The house of "Nioko Banco" is made of improved banco (with a thin layer of cement to protect the walls), the roof is made of sheet metal and the floor of cement. It consists of a single room and is located in a courtyard of three houses belonging to the same family. It serves as a guest room. It has a door and a louvre (nako) window on the same wall, opposite the wall where the logger was installed on the south-eastern side. The corresponding wall is not exposed to sunlight but shaded by the high wall surrounding the property. Much use is made of the courtyard where a large mango tree in the middle provides some shade for the inhabitants.
- The "Nioko Cement" building is a large three-room house, made of cement, with a ceramic tiled floor and sheet metal roof. The data logger was placed in the living room of 20 m^2, which has three windows with glass or trellis (nako) and two doors, with a high ceiling. It is therefore relatively well ventilated. The wall where the logger was placed faces south-west and is exposed to direct sunlight with no shade. The courtyard as a whole is unshaded. Six people live in this house, three adults and three children.
- The "Polesgo Cement" house has been inhabited since 2005 by a household whose main activity is brewing dolo, the local millet beer. It is a single-storey house, composed of a living room and a bedroom. The roof is sheet metal, the floor cement, and the walls simple banco. The logger was placed in the bedroom. There is a window and two small openings for ventilation around the window. The trellis window, made of iron nako, is opposite the entrance to the room, which is separated from the living room by a curtain. The wall where the logger was located faces south-west and is slightly shaded at the end of the day by a mango tree in the courtyard. Three people (two adults and a child) sleep in this room at night.
- "Polesgo Banco" is a single-storey house with a living room and a bedroom. The house is isolated in a large courtyard where there was only a 1.5 m-high tree at the time of the measurements. The roof of the house is made of sheet metal, the floor is cement and the walls are improved mud. In the living room where the temperatures were recorded, there is a trellis window made of iron nako, on the same side of the wall as the front door, and opposite the wall where the data logger was placed. There is no door between the bedroom and the living room, just an opening. The wall where the logger was located faces north-west, with no shading effect. When measurements began, only one person was living in this house. Then, during the measurement period, this person moved away, leaving the house unoccupied and unfurnished until the end of the period.
- Built according to ancestral techniques, the bioclimatic Nubian Vault in Somgandé is well insulated. It is made of stone, earth and water and is suitable for countries with hot, dry climates. The data logger was placed in the living room, with several windows and glass

doors allowing significant natural ventilation. The logger was placed on an east-facing partition wall. This is a guest house, located in a residential area, so there are many visitors. The courtyard is large, with some shade afforded by a few small trees (shorter than 2 m). During the day, the house itself is not shaded.

2.2 Regional climate monitoring and assessment

ERA-Interim reanalyses (Dee et al. 2011) are used to characterize the regional-scale climate context. Here, we make use of air temperature (daily minimum, maximum and mean air temperature at 2 m above the surface, hereafter referred to as Tn, Tx, T2m: °C), and wind at 10 m ($m.s^{-1}$). These variables are usually considered reliable because they are directly constrained by data assimilation. In addition, we also consider the total column water vapour content ($g.m^{-2}$) and shortwave radiation at the surface ($J.m^{-2}$), which are more dependent on the model physics and need to be considered with greater caution.

Observed records of air temperature (Tn and Tx: °C) are also available at the synoptic station of Ouagadougou (at the international airport, south of the city centre: Fig. 1). Although these time series include some missing values over the period considered in this work (only 161 Tn and 307 Tx values out of the 393 days of the study period, leaving 59% and 22% of missing values, respectively), such in situ data is used to assess the quality of ERA-I temperature and to correlate outdoor and indoor temperature variability (Supp. Figs. 1-2).

Land surface temperature (LST) estimates, derived from Landsat 8 OLI (Operational Land Imager), make it possible to obtain continuous temperature fields at a 100-m horizontal resolution over Ouagadougou and its surroundings. Such estimates are obtained at 10:25 UTC for 7 dates for which cloud cover is very weak or null (23 Nov. and 25 Dec. 2017; 10 Jan., 27 Feb., 15 Mar., 16 Apr. and 18 May 2018). Vegetative activity is derived from the same dataset at the same dates through a normalized difference vegetation index (NDVI: Fig. 1) at a 30 m resolution. For the purposes of illustration, Figure 3 shows the estimated LST fields at four dates chosen to represent the seasonality in LST, and the time evolution of spatial contrasts throughout the domain of interest. Both NDVI and LST were calculated using the QGIS Land Surface Temperature Estimation Plugin (Ndossi and Advan 2016). LST was obtained from the Radiative Transfer Equation of Sobrino et al. (2004) with corrections for atmospheric effects (Barsi et al. 2003) and land surface emissivity (Sobrino et al. 2008). In order to compare the indoor temperatures measured in the seven houses and LSTs in their surroundings, we considered various spatial scales representative of the neighbourhoods of the houses. To that end, we averaged spatially the LST values over pixels for buffers of different sizes, from the nearest neighbour (i.e. the Landsat pixel closest to the house) up to the 1000 m zone around the house of interest. Intermediate scales are also considered, through buffers of increasing size with a step of 100 m (i.e. buffers of 0, 100, 200, …, 900 and 1000 m around each house). Results revealed very low sensitivity to this choice (not shown). Thus, only the nearest neighbours are presented and discussed.

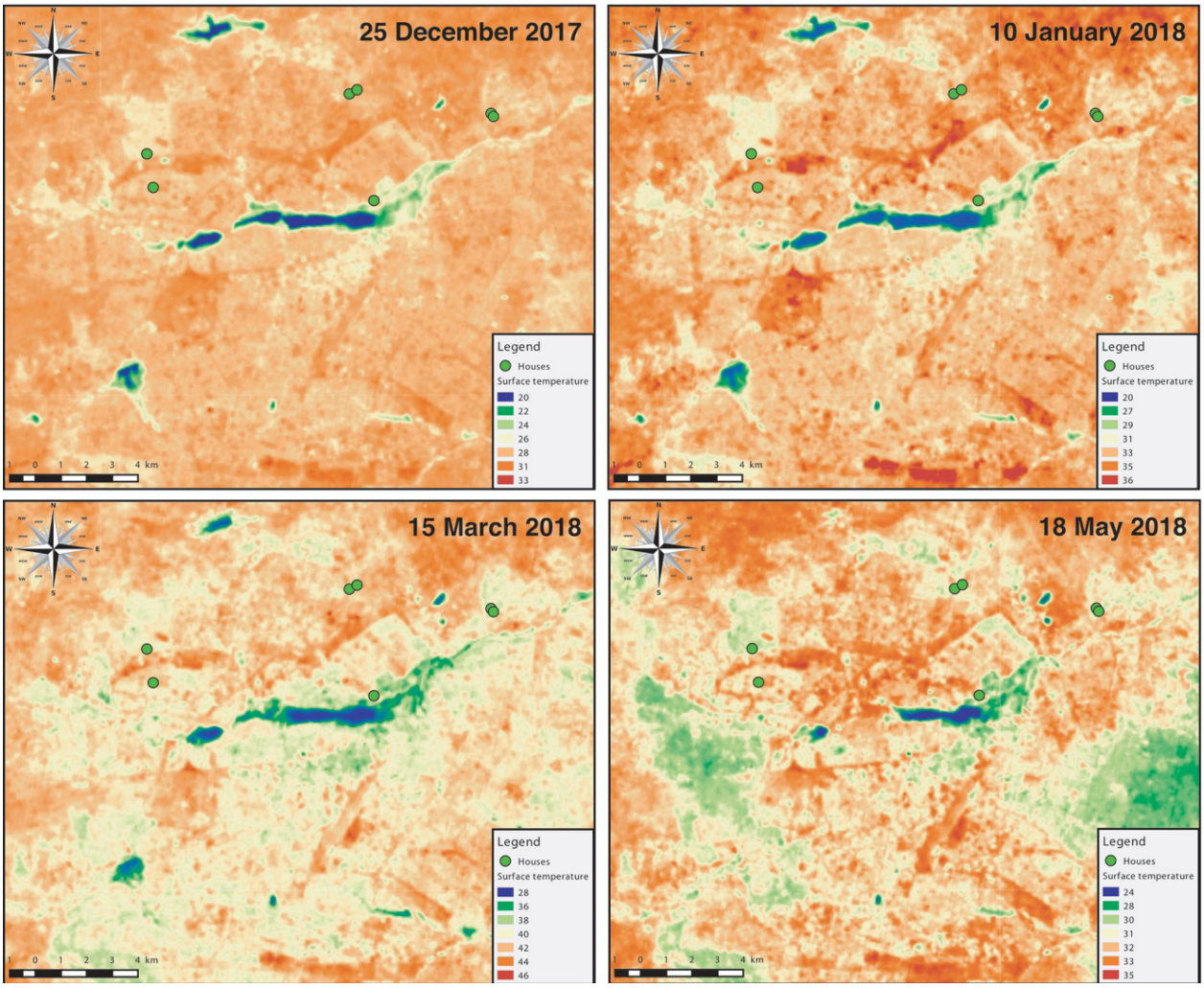

Figure 3 Land-surface temperature as derived from Landsat imagery, for four dates with little or no cloud cover. For readability, colour scales differ from one date to another: see legends for details. Green dots show the location of the seven houses analysed in this work.

3. Results

3.1 Different thermal signatures between houses

Figure 4 shows the average indoor temperatures recorded in the seven houses. The two-dimensional display of the time series provides an immediate visualization of the two orbital cycles driving temperature variability, that is, the diurnal and annual cycles. Over the study period, the average indoor temperature for all houses is 31.7 °C, denoting hot conditions that exceed by 3 °C the average outdoor air temperature recorded at the weather station over the same period (28.7 °C). This average value conceals very strong temporal variability. Daily peaks of temperature are recorded between 14:00 and 16:00 UTC throughout the year (with an overall maximum of 42.3 °C obtained when averaging the seven indoor records of 7 May 2015 at 15:00 UTC). Daily minima occur late at night and early in the morning, typically between 05:00 and 07:00 UTC, whatever the

season of the year (the overall minimum of 23.0 °C occurred on 22 December 2017 at 06:00 UTC). Seasonally, a bimodal cycle of temperature is found, with a main temperature peak in spring (March through May), i.e. before the onset of the monsoon, and a secondary, lower peak after the monsoon in autumn (October and November). Such temperature seasonality is also found in outdoor air temperature (Supp. Fig. 1) and is typical for the hinterland regions of the Sahel (Moron et al. 2016). In addition to these combined cycles, strong day-to-day temperature variability is also clearly discernible in these records (Fig. 4). Detailed analysis of individual time series of indoor temperature (Supp. Fig. 4) show in-phase daily fluctuations, denoting the strong control of larger-scale climate and weather on indoor temperature. This point is further addressed below.

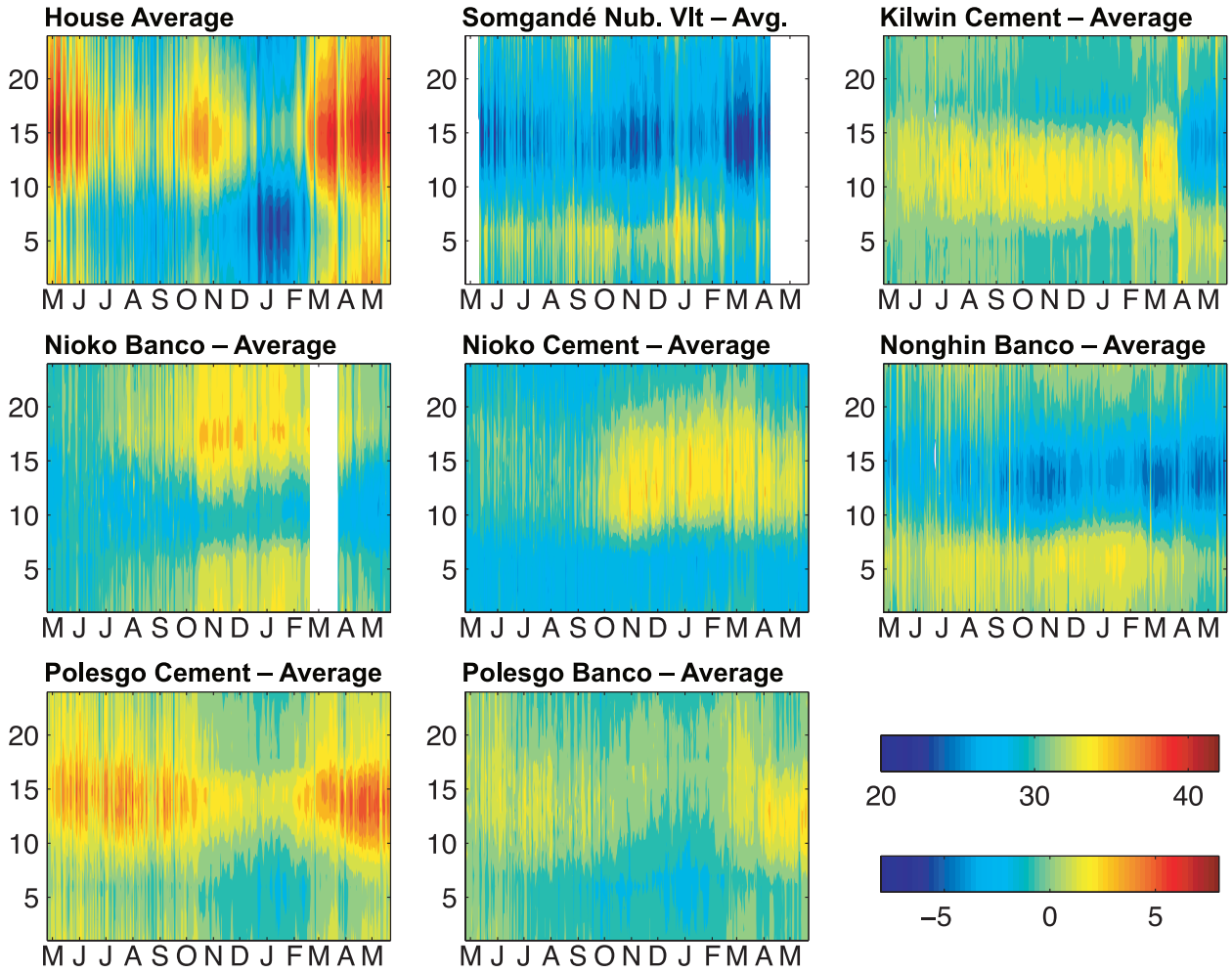

Figure 4 Daily vs. hourly indoor temperature diagrams for the recording period between 25 April 2017 and 22 May 2018. Upper left-hand diagram: average of hourly indoor temperatures (°C, upper colour legend). All other diagrams: indoor temperature differences between each house and the average (°C, lower colour legend).

Figure 4 also presents the particularities of each house with respect to the mean. Although the statistical robustness of the average should be questioned, due to the limited sample size (seven

houses only), analysing the difference between each house and their mean reveals a few salient points. (i) Even though it is the coolest house on average, the "Somgandé Nubian Vault" (Fig. 2a-b) stands out even more clearly in the afternoons (see Supp. Fig. 3), when indoor temperatures rise dramatically in most places but more moderately in this bioclimatic house, as a direct consequence of its shape (concentrating heat under the roof: Fig. 2b; Table 1) and design (materials with greater inertia). As an illustration, the maximum temperature recorded in Somgandé during the instrumented period is only 36.3 °C, on 19 March 2018. (ii) By contrast, the "Polesgo Cement" house (Fig. 2g) is, by far, the warmest, with the main departures from the mean concentrated in the afternoons. At this time of day, the temperature increases more strongly in this house than in any other building considered in this work, enhancing its distinctive thermal signature. The warmer the outdoor conditions, the greater the difference between this house and the others. This could entail major impacts for human health, all factors leading to heat stress and danger adding their effects. The overall temperature peak recorded in this house is 47.1 °C on 4 May 2018, which also corresponds to the highest temperature recorded in all seven houses over the period. (iii) All other houses exhibit intermediate behaviours between these extremes, but with very different diurnal and seasonal profiles. The "Nonghin Banco" house (Fig. 2d) is for instance rather close to the thermal signature of the "Somgandé Nubian Vault" bioclimatic house, albeit with slightly warmer conditions. It tends to exceed the average behaviour at night but is markedly cooler than other houses in the afternoon, under the warmest conditions, denoting thus a damped diurnal cycle and a narrower diurnal thermal range (DTR). The "Nioko Cement" house (Fig. 2e) has roughly the opposite signature, with a wider DTR amplifying temperature differences between the late night and the afternoon; overall, it is rather close to the house mean. The "Polesgo Banco" house (Fig. 2h) shares common properties with the "Nioko Cement" house, especially an above-average DTR. However, this particularity is also modulated by the seasonal cycle, and is more pronounced during the hot boreal spring than during the cold winter. Finally, the "Kilwin Cement" (Fig. 2c) and "Nioko Banco" houses (Fig. 2f) have almost reverse diurnal signatures, with "Kilwin Cement" being warmer than the average in the late morning and cooler during the late afternoon and at night, and "Nioko Banco" exhibiting exactly the opposite behaviour.

Such differentiation in the thermal profile of these houses, at the diurnal scale, can be related to many factors (e.g. house architecture, construction materials, surrounding environment – either built-up or not, indoor equipment, life habits and way of life: Table 1). Seasonal modulations in these particular signatures should be considered with caution. In "Kilwin Cement", the sudden change found in late March 2018 is caused by the installation of a ceiling fan in the bedroom where the thermometer was fitted. In "Nioko Banco" and "Nioko Cement", the sudden change in both houses between October and April (that is, after the monsoon retreat) is interpreted as denoting a particular signature of this northern neighbourhood of Ouagadougou. Unlike their counterparts in the temperate countries, large agglomerations of Africa are often characterized by quite weak night-time urban heat islands (Wienert and Kuttler 2005; Balogun et al. 2012; Ayanlade 2016; Scott et al. 2017). It is not certain if a clear and spatially coherent urban heat island forms at night in Ouagadougou, especially in the central parts of the agglomeration where large parks and water bodies (Fig. 1) can act to cool the urban boundary layer (Offerle et al. 2005; Lindén 2011). During the daytime, cooler conditions more often prevail in urban areas, because surface roughness enhances vertical mixing and turbulence, or because the weaker skyview factor increasing shading. Such effects are clearly visible in Figure 3, with LST differences of up to 5 °C between urbanized and nearby unbuilt parcels. Nioko being close to the northern boundary of the agglomeration (Fig.

1), we hypothesize that this neighbourhood is under the direct influence of the warmer rural air mass in winter, when northern wind regimes develop and prevail throughout the dry season (Cornforth et al. 2019).

3.2 Separating outdoor climate influence and architecture

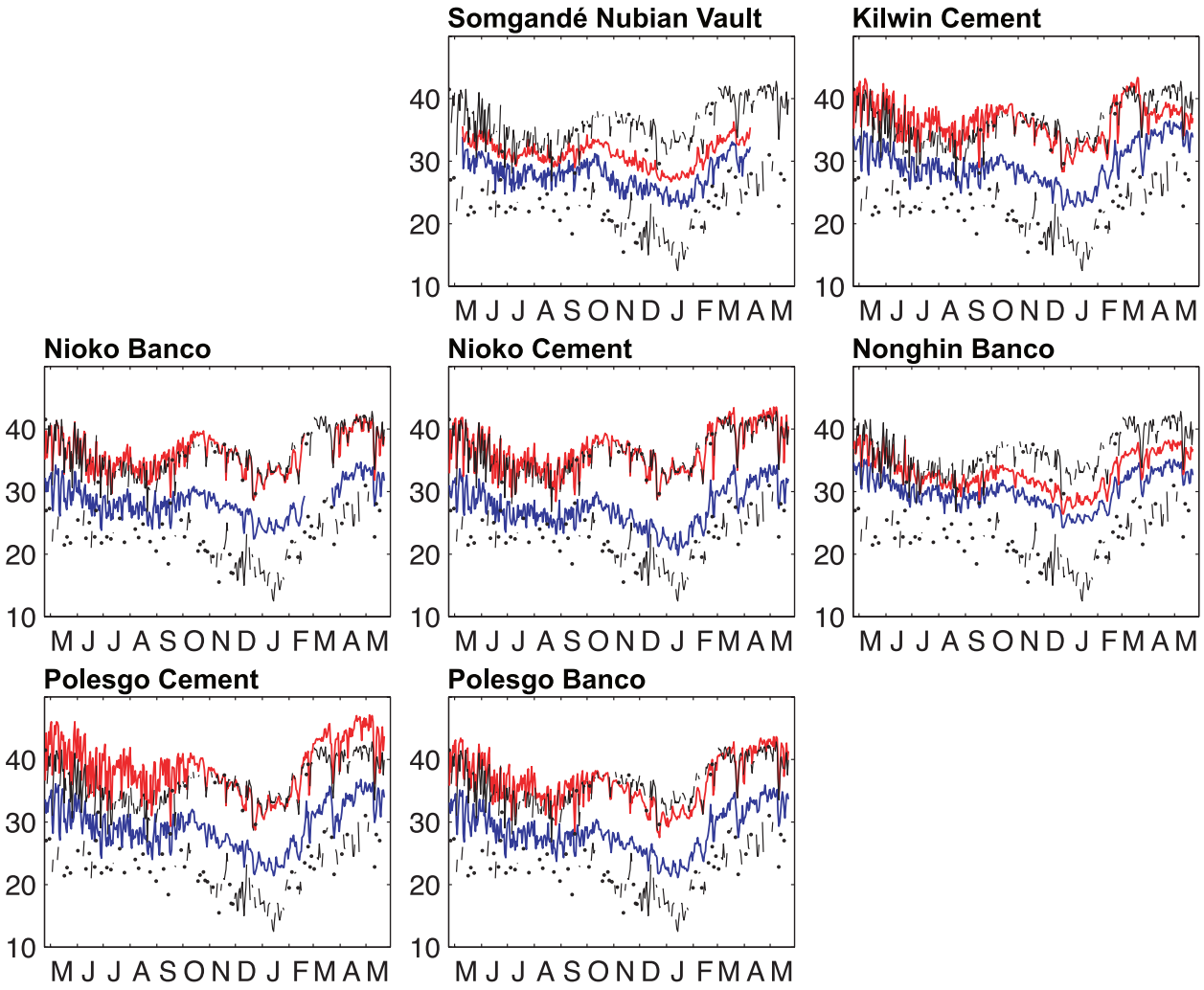

Figure 5 Daily minimum and maximum temperature at the synoptic weather station of Ouagadougou (black curves) and minimum (blue curves) and maximum (red curves) indoor temperature in each individual house.

Figure 5 aims to assess in detail the relationship between indoor and outdoor temperature. Here, the daily extrema of indoor temperature are plotted together with the Tn and Tx air temperatures recorded at the synoptic weather station of Ouagadougou international airport. For all houses, the general pattern of temperature is logically very similar indoors and outdoors, both for minimum and maximum temperatures. More importantly, these plots also reveal that, in all houses, the daily minimum temperature exceeds by 6 to 10 °C that recorded at the weather station: the thermal

inertia of the buildings mitigates the night-time radiative cooling. The "Nioko Cement" house experiences the coldest daily minima (and thus the smallest difference with Tn records), and "Nonghin Banco" the warmest minima. The results are more contrasted for daily temperature peaks, as suggested by the marked differentiation between houses already discussed in Fig. 4. Only the "Somgandé Nubian Vault" and "Nonghin Banco" houses have temperature maxima that are clearly below Tx records. Consequently, the inner DTR is also narrower for these houses, mostly because of these lower maxima. During the last two months of the period, the "Kilwin Cement" house exhibits similar behaviour, illustrating the major influence of the ceiling fan in lowering afternoon temperature peaks. The estimated temperature drop is typically 5 to 6 °C. Both "Nioko" houses display daily maxima that are almost identical to outer Tx values, throughout the study period (i.e., whatever the season of the year). They slightly exceed the temperature values recorded at the airport only in autumn and winter (October–January), an issue already discussed above that can probably be at least partly explained by the position of this neighbourhood within the agglomeration. Both "Polesgo" houses and "Kilwin Cement" before the installation of the fan in March 2018 tend to show inner peaks that exceed the Tx records during the hottest spring season, and also during the monsoon season in summer. This is particularly marked for the "Polesgo Cement" house from March to late October 2017. Inner temperatures often exceed the temperature of the human body, and they even recurrently exceed 40 °C. These results show that these houses are clearly different from the others during the seasons that are already the most difficult for the body to adapt to background heat (in spring) or humidity (in summer), dramatically enhancing the heat stress experienced by their inhabitants.

Are such differences between houses only modulated by their architecture (including their shape and construction materials) or do they relate also to specificities in outdoor conditions? The question can be raised for instance for the "Somgandé Nubian Vault" house, located close to the water reservoirs and a major forested urban park (Bangr Weogo). In order to take into account these potential effects of particular neighbourhood conditions, Figure 6 shows the differences between pairs of houses located in the same sector of the city. The main factor driving these differences is the architecture of the houses and possibly the built and green environment of the inner courtyard, since outdoor conditions are similar. Differences can reach 5 °C, the highest values being clearly found between 10:00 and 16:00 UTC, i.e. roughly during the diurnal temperature peak (Fig. 4 and Supp. Fig. 4). This is particularly meaningful, because this demonstrates the importance of architecture and construction materials in lowering indoor temperatures during the hottest hours of the day. Once again, the last two months of the Kilwin Cement time series should be considered with care, due to the installation of a fan completely changing the temperature in the room where the data logger was fitted. This further shows the potential usefulness of basic electrical equipment to reduce indoor heat stress (Uejio et al. 2011).

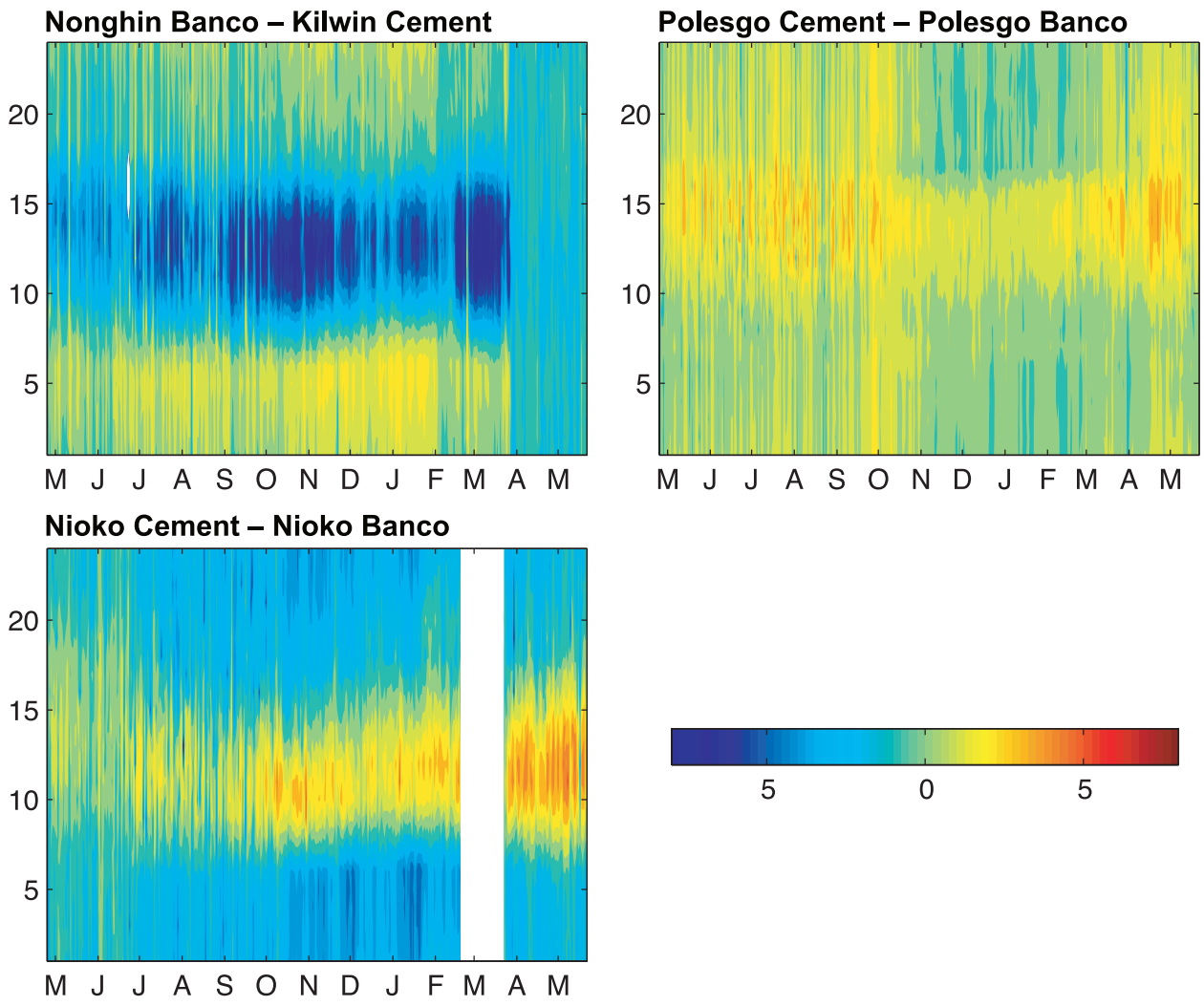

Figure 6 Daily vs. hourly diagrams of indoor temperature differences between pairs of houses in the same neighbourhoods (°C).

Unfortunately, this analysis does not make it possible to clearly state whether the particular signature of the bioclimatic Nubian Vault is partly inherited from outdoor conditions, since this house cannot be paired with another located close to it but architecturally different. In order to overcome this limitation of our campaign, Figure 7 presents scatterplots intersecting indoor temperature and LST close to the houses, for the seven dates at which Landsat data are available over Ouagadougou (i.e., clear-sky conditions). In order to help in interpreting these results, the same scatterplot (including 7 houses x 7 dates = 49 values) is duplicated to separate the spatial (Fig. 7a) and the temporal (Fig. 7b) variability. Although this figure only presents LST at the nearest grid-points, several tests were made by averaging satellite data over buffers of various sizes (up to 1000 m) centred on the seven houses considered in this work (see Section 2.2 for details). The results are remarkably consistent whatever the size of the buffer, denoting rather homogeneous LSTs close to the houses (Fig. 3).

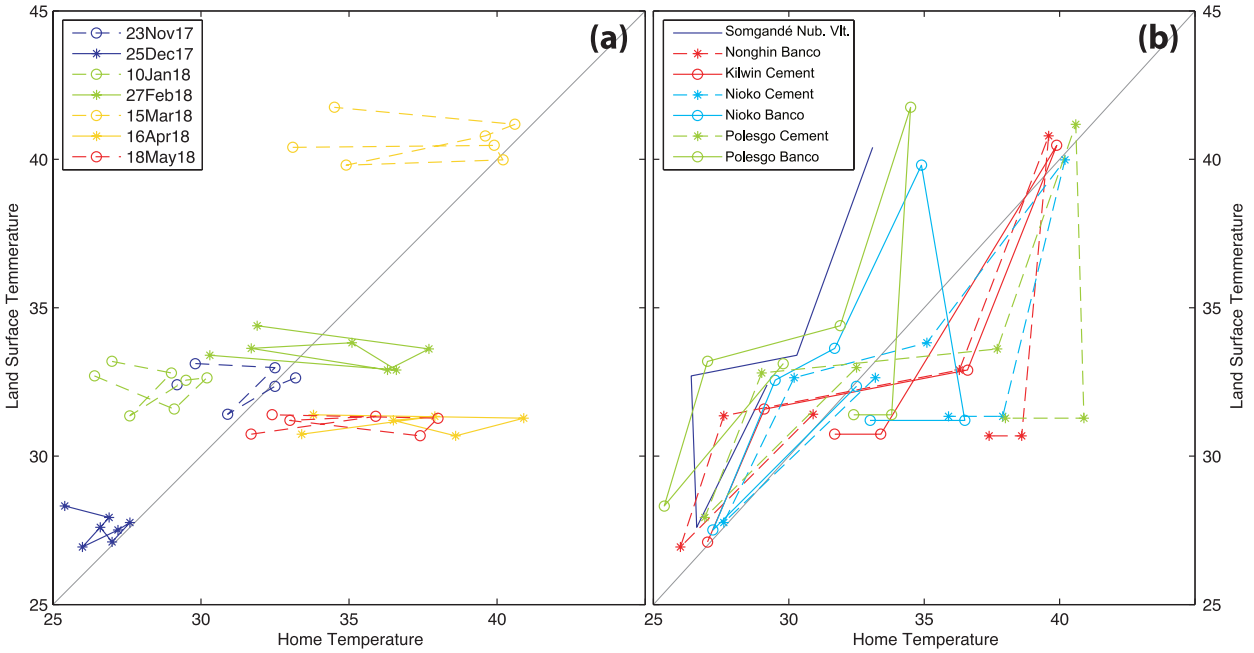

Figure 7 Comparison between land surface temperature derived from Landsat imagery vs. indoor temperature recorded at the same time. (a) Spatial variability: for each date (coloured curves), relationship between indoor and land surface variability for the seven houses and nearest Landsat grids. (b) Temporal variability: for each house and nearest Landsat grid, temporal changes of land surface and indoor temperature at the seven selected dates for which land surface temperature estimates are available.

Temporally (Fig. 7b), all the houses tend to show the same temperature changes from one Landsat date to another, an expected result driven by the seasonality of temperature (Fig. 5). It also shows that, at this time of the morning (10:25 UTC), the "Somgandé Nubian Vault" house is the only one that is systematically cooler than its surrounding outdoor LST. All other houses are quite close to the y=x line, which is quite coherent for this time of day. The largest departures from the first bisector are recorded for the late spring scenes (Fig. 7a), during the warmest season; they are particularly marked at "Polesgo Cement", already found to be the warmest house, and, more surprisingly, for "Nonghin Banco", which is usually rather cool (Fig. 4). For the latter, our hypothesis is that this particular behaviour is due to its strong thermal inertia, the warm indoor conditions in the morning being due to reduced night-time cooling (Fig. 4).

There is probably more interest in analysing the spatial variability (Fig. 7a). Whatever the date of the Landsat scenes, indoor temperature shows more variability than the corresponding LST estimations (LST itself being much more variable spatially than outdoor air temperature). For a given day, the standard deviation of indoor temperatures (from one house to another) ranges from 1.59 (25 December 2017) to 7.46 (16 April 2018), which is greater than that computed between corresponding Landsat pixels of LST estimates. While LST shows rather constant spatial variability, weakly modulated by the seasonal cycles (at least for the pixels nearest to the seven houses: Fig. 7b), indoor variability increases greatly with outdoor temperature, leading to larger differences close to the annual peak of temperature. This is particularly marked for the last two dates (April and May 2018) in Fig. 7a, for which the indoor records in the "Somgandé Nubian

Vault" house were missing (thus probably underestimating the indoor temperature variability from one house to another).

These results demonstrate that, when the annual temperature peak occurs and can cause major public health issues, temperature is also highly variable from one type of house to another. Thus, architecture and construction materials, as well as the built and green environment of the courtyard, can have a major influence in modulating (i.e., reducing or enhancing) the heat exposure and hence the heat stress experienced by the human body during this critical season. Severe climatic conditions are shown, here, to amplify the inequalities in the living conditions of the populations, a statement that could be of even greater importance as climate change continues.

3.3 Building response to abrupt temperature changes

In this section, we focus more particularly on abrupt temperature changes and characterize the buildings' response to such perturbations in outdoor conditions. Even though outdoor day-to-day temperature variability is generally lower than in the mid-latitudes, the physical processes driving such temperature variability at short to seasonal scales across the Sahel are now well understood (e.g., Guichard et al. 2009; Fontaine et al. 2013; Moron et al. 2016, 2018; Oueslati et al. 2017; Barbier et al. 2018; Sambou et al. 2020). For data availability reasons (Sect. 2.2) and because houses differ more in the afternoon under the hottest diurnal and seasonal conditions (Sect. 3.1 and 3.2), we focus here on abrupt changes in Tx, as recorded at the synoptic weather station of Ouagadougou airport. We first calculate day-to-day Tx changes (i.e., ∂Tn / ∂t) and verify that reanalyses are not only skilful for estimating day-to-day temperature variability (in spite of a clear underestimation of the DTR due to systematic warm Tn and cold Tx biases: Supp. Fig. 1), but also the magnitude of their day-to-day changes (Supp. Fig. 2). The computation of these day-to-day differences being based on two consecutive non-missing values, the number of possible calculations over our 393-day long study period drops to 240 for Tx, against only 78 for Tn (Supp. Fig. 2).

Here, we choose to focus on the most abrupt decrease in Tx, by removing the 5% lowest ∂Tn / ∂t values. Twelve such Tx drops are removed. Similar analyses have been applied to abrupt increases in Tx (using the 5% highest ∂Tn / ∂t values) and lead to qualitatively similar conclusions (modulo a reversed sign for temperature changes) in terms of thermal inertia of the houses (not shown). However, over our study period, positive ∂Tn / ∂t values are weaker than their negative counterparts (barely exceeding +5 °C: Supp. Fig. 2), acting thus to reduce the magnitude of outdoor and indoor temperature response to these perturbations (not shown).

Figure 8a shows that the local Tx changes recorded at Ouagadougou seem to show some spatial coherence over the central Sahel, a statement that should be considered with care since it may vary strongly from one event to another and be perturbed by the anisotropic distribution of weather stations assimilated in the reanalyses. Determining the spatial extent of these daily Tx fluctuations is not our primary purpose here. Fig. 8a also shows that these changes are not associated with strong and consistent modifications in regional atmospheric circulation. The decrease in Tx corresponds rather to a significant decrease in shortwave solar radiation reaching the surface over and around Ouagadougou (Fig. 8b) and, more locally, a significant increase in the total water vapour in the air column (Fig. 8c). Taken together, these results suggest that the decrease in Tx is

mostly due to changes in the radiative budget of the atmosphere, possibly due to cloud cover or aerosols, confirming the processes shown to control Tx variability over the Sahel region (Oueslati et al. 2017; Moron et al. 2018).

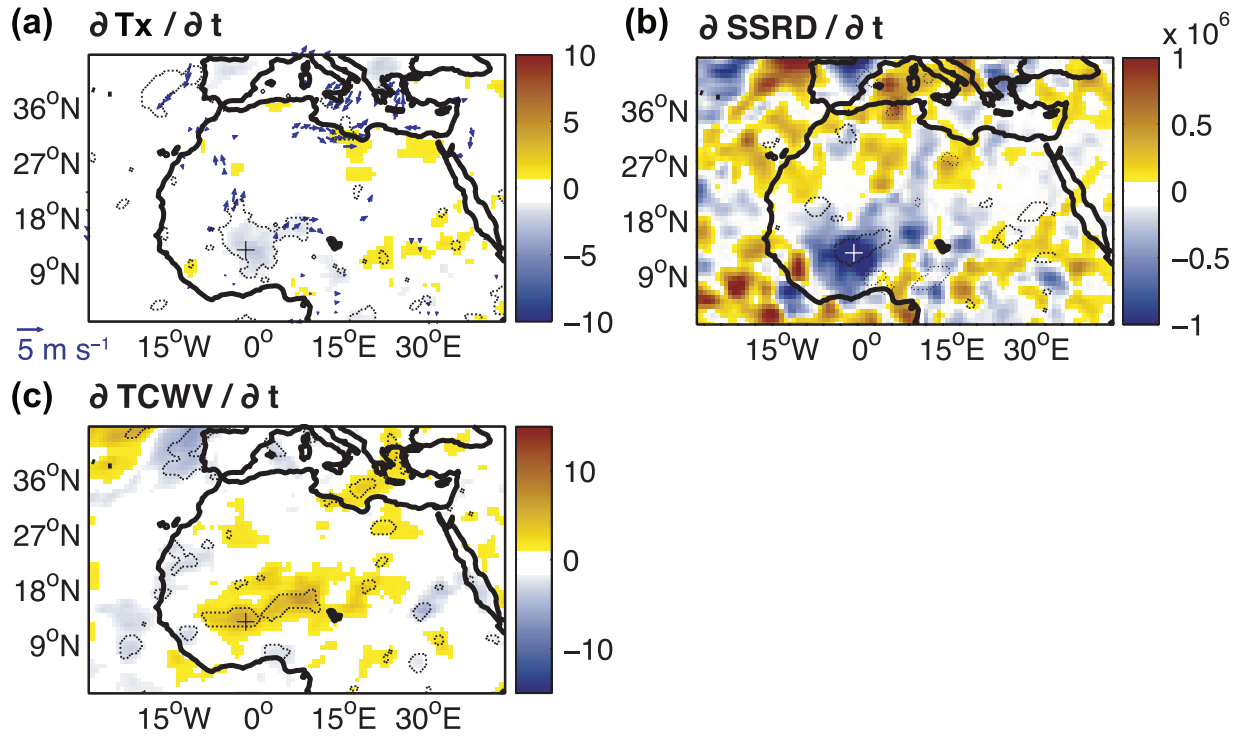

Figure 8 Abrupt decrease in Tx outdoor air temperature, and associated regional-scale mechanisms. (a) Changes in maximum air temperature at 2 m above ground level (Tx, in °C) and horizontal wind (m.s^{-1}) at 10 m between the day before and the day of the abrupt decrease in Tx (d_1 minus d_0). Dashed curves show statistically significant changes according to a t-test at the 95% confidence level. All fields are from ERA-Interim reanalysis. The plus sign shows the location of Ouagadougou. (b) As (a) but for downward solar radiation at the surface at 15:00 UTC (J.m^{-2}). (c) As (a) but for total water vapour integrated vertically on the air column at 15:00 UTC (g.m^{-2}).

For 4 out of the 12 abrupt Tx decrease events identified, Figure 9 shows (i) the Tx day-to-day changes at Ouagadougou airport (used to detect these events), (ii) corresponding daily Tx changes in ERA-Interim, and (iii) hourly temperature evolutions in the seven houses considered in this work. These dates are chosen because they are representative of the typical changes in indoor temperature during abrupt Tx variations and also because they occur during or close to the warmest season of the year, that is, late spring (Supp. Fig. 1). By construction, Tx records at the synoptic weather station display a drop of typically 5–7 °C between day #0 and day #1, an evolution generally reproduced by ERA-Interim, although of less amplitude. Reanalyses also display their systematic cold bias prevailing in the afternoon (Supp. Fig. 1). Between days #1 and #2 temperature changes are highly variable from one event to another, indicative of weak serial correlation in the ∂Tn / ∂t values.

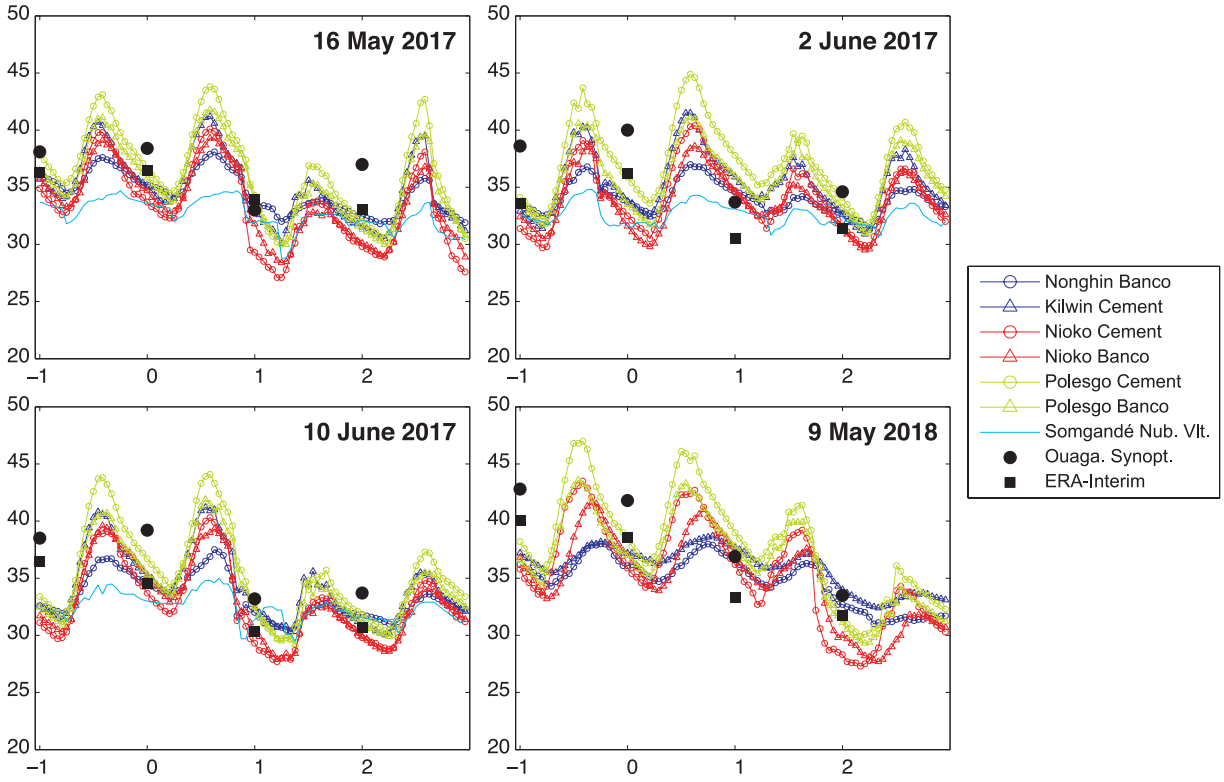

Figure 9 Illustration of four (out of 12) selected abrupt decreases in Tx. Black dots: day-to-day changes in Tx according to the Ouagadougou synoptic station (used to detect largest Tx changes). Abrupt changes occur between d_0 and d_1. Black squares: the same for ERA-Interim. Colour curves: hourly indoor temperature records in the seven houses.

Detailed analysis of indoor response to these changes in the regional climate (Fig. 9) first confirms the very high variability of temperature from one house to another. This is especially true for indoor DTR, that mostly leads to smoothing or modulation of the afternoon peak. Houses with low DTR like "Somgandé Nubian Vault" or, to a lesser extent, "Nonghin Banco", clearly show a strongly damped afternoon peak, while their night-time minima are close to the average values of the houses. Overall, these houses are therefore cooler than the others. Some houses like "Polesgo Cement" or "Polesgo Banco" are generally warmer than the others whatever the time of day, illustrating that the DTR and the thermal inertia of the houses are not the only factors influencing maximum indoor temperatures. The abrupt Tx decrease between day #0 and #1 is accompanied by indoor temperature changes of almost identical magnitudes. This is especially true for day-to-day changes in the afternoon temperature peak, except once again for the "Somgandé Nubian Vault" and "Nonghin Banco" houses. This shows that most houses respond strongly and rapidly to changes in outdoor climate conditions (a result that is confirmed for both increases and decreases in Tx and Tn: not shown). Such rapid adjustments of indoor thermal conditions to weather and climate variability could be indicative of the importance of daytime shortwave radiation in heating the house interiors. However, it was not easy to identify relationships between radiation and indoor temperature based on our sample and a rather short instrumented campaign. This was because radiation seems to control both indoor and outdoor temperature, thus leading to differences between indoor and outdoor temperature that are mostly season-dependent (as shown by Fig. 5)

and, thus, less related to short-lived changes in shortwave radiation (not shown). By contrast, the coolest houses, with greater inertia, are also those that show the smallest changes from one day to another, a result that is also confirmed for sudden temperature (Tx or Tn) increases (not shown). Under current climate conditions, Sahelian HWs are rather short (Moron et al. 2016; Ringard et al. 2016; Oueslati et al. 2017) and houses with strong thermal inertia could help mitigate both heat exposure and heat stress associated with such phenomena.

3.4 Building-dependent heat exposure

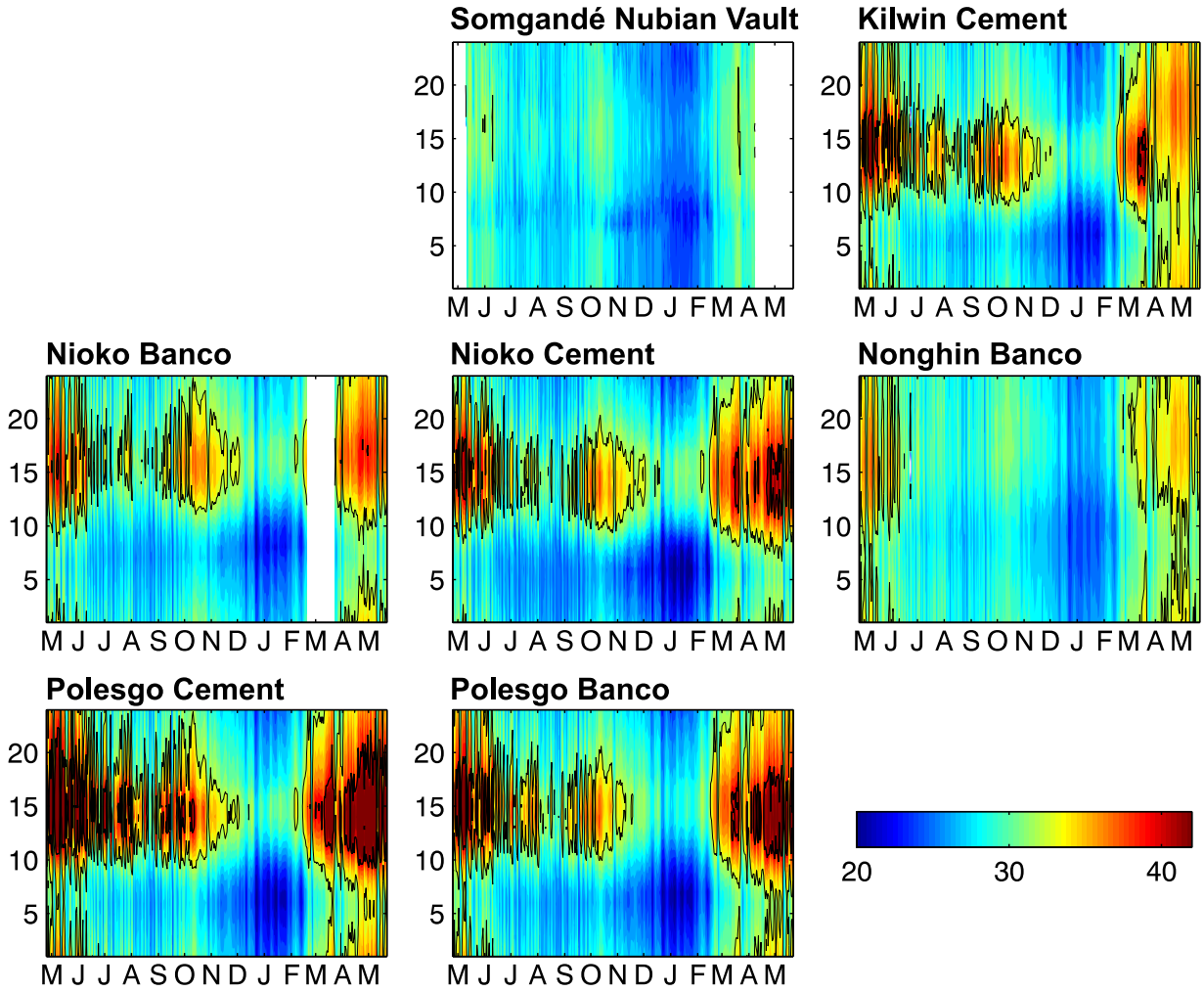

Figure 10 Daily vs. hourly diagrams of indoor heat index for the recording period between 25 April 2017 and 22 May 2018. Thin black contours show the "Extreme Caution" threshold. Thick black contours show the "Danger" threshold.

By mitigating or enhancing the extreme temperature peaks recorded at Ouagadougou in the afternoon, the built environment has the potential to modulate the heat exposure of its inhabitants (Ayanlade et al. 2019; Tyubee et al. 2020). Overall heat index (HI) variability and associated thresholds (extreme caution and heat danger) in the seven houses is shown in Fig. 10. Table 2 presents the time spent, in each house and over the study period, in each HI heat stress category.

The same thresholds (Steadman 1979) are also identified in Fig. 10 in order to visualize the time distribution of associated thresholds crossings.

	Somgandé Nubian Vault	Kilwin Cement	Nioko Banco	Nioko Cement	Nonghin Banco	Polesgo Cement	Polesgo Banco
Caution	7970	6743	6740	7169	8072	5933	6727
Extreme Caution	30	2537	1919	2066	1343	2668	2289
Danger	0	134	14	180	0	813	399
Extreme Danger	0	0	0	0	0	1	0
Σ	8000	9414	8673	9415	9415	9415	9415

Table 2 Duration (number of hours) spent in each heat index category (rows) based on indoor temperature and humidity records (columns). The total number of values available during the recording period between 25 April 2017 and 22 May 2018 is also indicated.

Although the first category ("caution", for which no major health issues are expected) is clearly predominant for all houses (because the whole year is considered here, including the winter season), the difference from one house to another is striking in terms of occupation of the potentially dangerous (i.e. the upper two) categories. The "coolest / highest inertia" houses ("Somgandé Nubian Vault" and "Nonghin Banco") are totally absent from these categories, leading to reduced heat stress and danger for their inhabitants. The "Somgandé Nubian Vault" house is confined to the "caution" category, except for 30 hours spent in the second one ("Extreme Caution"), a value that already exceeds 1300 hours at "Nonghin Banco". These results tend to confirm the singular behaviour of the bioclimatic house, but it should be observed that the final weeks of recordings (Spring 2018) are missing for the "Somgandé Nubian Vault" house, which could reduce the time spent in the "Extreme Caution" category during the annual peak of temperature, and thus alter the comparison with the other houses. As expected, the warmest house ("Polesgo Cement") is also the one most present in the upper categories, with more than 800 hours in "Danger" and even one hour in the "Extreme Danger" category, materializing the immediate risks of deadly heat. The situation is particularly critical during in late spring (May and June: Fig. 10), for which the whole day and night is likely to exceed the "Extreme Caution" threshold, and most of daytime is in the "Danger" category (for at least 5–8 consecutive hours, i.e. typically between 10:00–12:00 and 18:00–20:00 UTC). All other houses exhibit intermediate behaviours, and are notably present 14 hours ("Nioko") to roughly 400 ("Polesgo Banco") in the "Danger" category. This indicates potentially very serious health issues in most of the houses considered in this work. The frequency and occurrence of the "Danger" and even "Extreme Danger" categories are expected to rise significantly in coming decades under climate change, raising the question of public health impacts of climate extremes, especially heat extremes and HWs (e.g., Ringard et al. 2016; Moron et al. 2016; Sambou et al. 2021). The most underprivileged populations face the greatest difficulties in protecting themselves against deadly heat during such severe events,

confirming that climate change enhances inequalities and differences between the most and least resilient households.

4. Discussion

Using hourly air temperature and humidity records performed over a 13-month period in seven houses of Ouagadougou, Burkina Faso, this pilot study led to the following main results.

— Indoor temperature is much more variable, from one house to another, than corresponding land surface temperature near the houses, as estimated by satellite imagery. This shows the primary importance of house architecture and the nearby environment, and that of indoor activities and inhabitants' habits, for modulating indoor temperatures. The installation of a ceiling fan in one of the houses, which had not been planned for in the instrumented campaign, reveals the influence of such devices for modifying indoor thermal conditions (temperature peaks reduced by 5–6 °C). It also illustrates the importance of having access to metadata to avoid erroneous interpretations of collected time series.

— Differences from one house to another are particularly marked during the hottest hours of the hot season, i.e. in spring afternoons (May–June). Houses with high thermal inertia greatly smooth the diurnal temperature peak, reducing the heat exposure of their inhabitants. This implies that houses exacerbate differences in living conditions and heat stress and danger experienced by their occupants. For illustrative purposes, the hottest house experienced an overall temperature maximum that exceeded by nearly 11 °C that of the coolest house (47.1 °C in "Polesgo Cement", as against 36.3 °C in "Somgandé Nubian Vault"). These maxima have not been reached at the same time, indicating that houses show contrasted responses to outdoor climate variability.

— Most houses display fast and strong responses to changes in outdoor weather and climate conditions (temperature, radiation, wind, etc.). This statement is confirmed at different timescales, including the annual and diurnal cycles, but also for day-to-day variability. Houses with the greatest thermal inertia are also those exhibiting weaker dependency on outdoor conditions. By smoothing the afternoon temperature peaks, they protect their occupants from deadly heat.

The recent instrumented campaign is planned to end with a presentation of the results obtained in this study to the households involved in the study.

5. Conclusion

This work revealed huge difficulties in obtaining reliable, homogeneous and comparable indoor temperature time series over the long term. Our results also show how complex the issue of indoor temperature may be, and how critical the problem of heat danger may become in the Sahel in the near future.

There are numerous degrees of freedom modulating indoor temperature, including but not limited to (i) architecture (the size and shape of the buildings and their inner rooms, the size and

arrangement of doors and windows determining natural ventilation, construction materials, the width of walls and [lack of] insulation of roofs, etc.); (ii) indoor equipment (including fans, electrical or electronic devices, etc.) conditioned themselves on the availability or urban infrastructures like electricity and, more generally, the habits and way of life of the households; and (iii) outdoor conditions, either regional (weather and climate conditions, especially air temperature, solar radiation, wind speed and direction) or local (especially the skyview factor, determining the presence or absence of shading effects and thereby the radiation received by the buildings, but also their location within the agglomeration). The present work did not allow for a quantitative and precise assessment of the relative weight and role of each of these parameters: such was not the purpose of this pilot study. Much more ambitious campaigns with longer acquisition periods are now needed to disentangle the respective influence of these factors.

From a building point of view, increasing the number of houses considered could allow for a more detailed quantification of the aforementioned parameters. Through a strategy focusing on contrasted houses located in the same neighbourhoods, it could also further help to separate indoor vs. outdoor influences. A major difficulty noted for this work was to have the data loggers accepted by the inhabitants, ideally in the bedroom along the north-facing wall to reduce direct radiation. It proved unfeasible to apply this criterion systematically in the present work because most people were reluctant to participate in this survey, and even the volunteers chose convenient places to install the data logger as a mandatory condition for their agreement. It is expected that non-negligible uncertainties may be associated with the localization of the data logger within the houses, an issue that remains to be quantified.

From a climatic point of view, longer campaigns using both indoor and outdoor measurements of air temperature, could help assess the role of outdoor conditions, especially solar radiation and air temperature, with increased robustness. Here, radiation was found to have a significant, yet complex influence, that could not be fully determined because of quite short time series and strong co-linearity with other climate variables (temperature, humidity, etc.) equally modulated by the annual and diurnal cycles. Surface solar radiation is found to increase both indoor and outdoor temperature, and, in our study period and based on our sample of seven houses, it seems to modulate quite weakly the temperature differences between indoors and outdoors. A particular case is the Somgandé Nubian Vault, this bioclimatic house being built to remain quite cool even under hot outdoor conditions. In this case, the temperature gradient is more pronounced under strong radiative conditions, with outdoor temperature increasing more than indoor temperature in this house.

The exacerbated contrasts, from one house to another, of indoor thermal conditions during the hottest hours of the warm season, is one of the key findings of this study. It could have major implications for future work and, more importantly, for local populations, raising the question of the impacts of temperature and heat exposure on human health. During the hot spells or HWs, indoor and outdoor temperature peaks combine their effects and are likely to cause major public health issues, excessively detrimental to the poorest populations. This is especially true in the already hot Sahelian belt, especially in spring. Other detrimental impacts are also expected in living, working and learning conditions. Such problems are of increasing importance with ongoing climate change.

Projections of indoor temperature conditions could become feasible, once a robust sample of indoor temperature is obtained and once the relative weight of outdoor climate variables is assessed. This could be achieved for contrasted houses, e.g. through multivariate transfer functions between projected outdoor climate and indoor conditions. Eventually, one could estimate the time evolution of potentially dangerous conditions for human health, using bioclimatic indices and associated danger thresholds. Such results could raise the question of the permanent habitability of hinterland Sahelian regions and cities by human communities in the future.

Strategies to mitigate and adapt to climate change in tropical Africa could finally include, in addition to low-carbon development and economies, major efforts for sustainable and energy-efficient urbanization. This would be a drastic change from current settlements in many informal areas of major African cities. And yet a necessary change, to help populations resist and protect against the rapidly-increasing risk of deadly heat. Simple electric devices like ceiling fans act to reduce indoor temperature, but their generalization would imply a surge in energy demand. The example of the bioclimatic house considered in this work ("Nubian Vault") shows that carbon-free solutions are equally efficient in reducing heat exposure with no additional energy consumption, thereby contributing to the "no regret measures" increasingly and urgently needed in our warming world.

CRediT authorship contribution statement

BP: Formal analysis; Methodology; Investigation; Visualization; Writing. **SDS**: Conceptualization; Data curation; Investigation; Writing. **GMB**: Writing - review & editing. **YC**: Data curation. **KD**: Data curation. **JDD**: Methodology; Visualization; Writing - review & editing. **AS**: Data curation. **SJ**: Funding acquisition; Writing - review & editing.

Declaration of competing interest

The authors declare that they have no known competing financial interests or personal relationships that could have appeared to influence the work reported in this paper.

Acknowledgments

The authors are deeply grateful to the households in Ouagadougou that accepted to participate in this experimental study. They also thank Ms. Jeanne-Louise Pernette who helped analyse the satellite data used in this work. This study is part of ANR Project ACASIS (2014–18; Grant ANR13-SENV-0007) and I-SITE Bourgogne Franche-Comté Junior Fellowship IMVULA (AAP2-JF-06). Calculations were performed using HPC resources from DNUM CCUB (Centre de Calcul de l'Université de Bourgogne). The authors dedicate this work to Dr. Françoise Guichard who passed away when this paper was still in progress, and with whom the lead authors had constructive and intense discussion about the climate of West Africa.

References

Adesina J.A., Piketh S.J., Qhekwana M., Burger R., Language B., Mkhatshwa G. (2020) Contrasting indoor and ambient particulate matter concentrations and thermal comfort in coal and non-coal burning households at South Africa Highveld. *Science of The Total Environment*, 699, 134403. doi:10.1016/j.scitotenv.2019.134403.

Adunola, A.O. (2014) Evaluation of urban residential thermal comfort in relation to indoor and outdoor air temperatures in Ibadan, Nigeria. *Building and Environment*, 75, 190-205. doi:10.1016/j.buildenv.2014.02.007.

Ahmadalipour A., Moradkhani H., Kumar M. (2019) Mortality risk from heat stress expected to hit poorest nations the hardest. *Climatic Change*, 152(3-4): 569-579. doi:10.1007/s10584-018-2348-2

Anderson G.B., Bell M.L., Peng R.D. (2013) Methods to Calculate the Heat Index as an Exposure Metric in Environmental Health Research. *Environmental Health Perspectives*, 121 (10):1111-1119. doi:10.1289/ehp.1206273

Ayanlade A. (2016) Seasonality in the daytime and night-time intensity of land surface temperature in a tropical city area. *Science of the Total Environment* 557–558 (2016) 415–424. doi:10.1016/j.scitotenv.2016.03.027

Ayanlade A., Esho O.M., Popoola K.O., Jeje O.D., Orola B.A. (2019) Thermal condition and heat exposure within buildings: Case study of a tropical city. *Case Studies in Thermal Engineering*, 14:100477. doi:10.1016/j.csite.2019.100477.

Balogun I.A., Balogun A.A., Adeyewa Z.D. (2012). Observed urban heat island characteristics in Akure, Nigeria. *African Journal of Environmental Science and Technology*, 6(1), 1-8.

Barbier J., Guichard F., Bouniol D., Couvreux F., Roehrig R. (2018) Detection of intraseasonal large-scale heat waves: characteristics and historical trends during the Sahelian spring. *Journal of Climate*, 31:61–80. https://doi.org/10.1175/JCLI-D-17-0244.1

Barsi J.A., Barker J.L., Schott J.R. (2003) An atmospheric correction parameter calculator for a single thermal band earth-sensing instrument. 2003 *IEEE International Geoscience and Remote Sensing Symposium. Proceedings*, 5:3014–3016. doi:10.1109/IGARSS.2003.1294665

Bazo J., Singh R., Destrooper M., Coughlan de Perez E. (2019) Chapter 18 - Pilot Experiences in Using Seamless Forecasts for Early Action: The "Ready-Set-Go!" Approach in the Red Cross. In A.W. Robertson and F. Vitart (Ed.), *Sub-Seasonal to Seasonal Prediction* (pp. 387-398). Elsevier. https://doi.org/ 10.1016/B978-0-12-811714-9.00018-8

Cornforth R., Parker D.J., Diop-Kane M., Fink A.H., Lafore J.P., Laing A., Afiesimama E., Caughey J., Diongue-Niang A., Kassimou A., Lamb P., Lamptey B., Mumba Z., Nnodu I., Omotosho J., Palmer S., Parrish P., Razafindrakoto L., Thiaw W., Thorncroft C., Tompkins A. (2019) The First Forecasters' Handbook for West Africa. *Bull. Amer. Meteor. Soc*., 100:2343–2351. doi:10.1175/BAMS-D-16-0273.1

Costello A., Abbas M., Allen A., Ball S., Bell S., Bellamy R., Friel S., Groce N., Johnson A., Kett M. (2009) Managing the health effects of climate change: lancet and University College London Institute for Global Health Commission. *The Lancet,* 373 (9676):1693-1733

Dapi L.N., Rocklöv J., Nguefack-Tsague G., Tetanye E., Kjellstrom T. (2010) Heat impact on schoolchildren in Cameroon, Africa: potential health threat from climate change. *Global Health Action,* 3 (1):5610. doi:10.3402/gha.v3i0.5610

Dee D.P., et al. (2011) The ERA-Interim reanalysis: Configuration and performance of the data assimilation system. *Quart. J. Roy. Meteor. Soc.*, 137:553–597. doi:10.1002/qj.828

Diedhiou A., Bichet A., Wartenburger R., Seneviratne S.I., Rowell D.P., Sylla M.B., Diallo I., Todzo S., Toure N.E., Camara M., Ngatchah B.N., Kane N.A., Tall L., Affhilder F. (2018) Changes in climate extremes over West and Central Africa at 1.5°C and 2°C global warming. *Environmental Res. Letters*, 13:6. doi:10.1088/1748-9326/aac3e5

Dirmeyer, P.A., Ford T. W. (2020) A Technique for Seamless Forecast Construction and Validation from Weather to Monthly Time Scales. *Mon. Wea. Rev.,* 148, 3589–3603, https://doi.org/10.1175/MWR-D-19-0076.1.

Dos Santos S. (2019) Les conditions environnementales de vie. In C. Rossier, AB Soura, G. Duthé (Ed.) *Inégalités de santé à Ouagadougou* (pp. 101-120). Paris: Ined Editions.

Fontaine B., Janicot S., Monerie, P.A. (2013) Recent changes in air temperature, heat wave occurrences, and atmospheric circulation in northern Africa. *Journal of Geophysical Research: Atmospheres*, 118:8536–8552. Doi:10.1002/jgrd.50667

Franco P., Szliwowski H., Dramaix M., Kahn A. (2000) Influence of Ambient Temperature on Sleep Characteristics and Autonomic Nervous Control in Healthy Infants. *Sleep*, 23 (3):1-7. doi:10.1093/sleep/23.3.1g

Gasparrini A., Guo Y., Hashizume M., Lavigne E., Zanobetti A., Schwartz J., Tobias A., Tong S., Rocklöv J., Forsberg B., Leone M., De Sario M., Bell M.L., Guo Y-L.L., Wu C-F., Kan H., Yi S-M., de Sousa Zanotti Stagliorio Coelho M., Saldiva P.H.N., Honda Y., Kim H., Armstrong B. (2015) Mortality risk attributable to high and low ambient temperature: a multicountry observational study. *The Lancet,* 386 (9991):369-375. doi:10.1016/S0140-6736(14)62114-0

Gough K.V., Yankson P.K.V., Wilby R.L., Amankwaa E.F., Abarike M.A., Codjoe S.N.A., Griffiths P.L., Kasel R., Kayaga S., Nabilse C.K. (2019) Vulnerability to extreme weather events in cities: implications for infrastructure and livelihoods. *Journal of the British Academy*, 7(s2):155–181. doi:10.5871/jba/007s2.155

Guichard F., Kergoat L., Mougin E., Timouk F., Baup F., Hiernaux P., Lavenu F. (2009) Surface thermodynamics and radiative budget in the Sahelian Gourma: Seasonal and diurnal cycles. *J. Hydrol*., 375:161–177. doi:10.1016/j.jhydrol.2008.09.007

Intergovernmental Panel on Climate Change (2013) *The Physical Science Basis. Contribution of Working Group I to the Fifth Assessment Report of the Intergovernmental Panel on Climate Change*. Cambridge and New York: Cambridge Univ. Press.

Kunutsor S.K., Powles J.W. (2010) The effect of ambient temperature on blood pressure in a rural West African adult population: a cross-sectional study. *Cardiovascular Journal of Africa*. 21 (1):17-20

Larrieu S., Carcaillon L., Lefranc A., Helmer C., Dartigues J-F., Tavernier B., Ledrans M., Filleul L. (2008) Factors associated with morbidity during the 2003 heat wave in two population-based cohorts of elderly subjects: PAQUID and Three City. *European Journal of Epidemiology,* 23 (4):295-302

Lavaysse C. (2015) Warming trends: Saharan desert warming. *Nature Climate Change*, 5:807–808.

Lindén J. (2011) Nocturnal Cool Island in the Sahelian city of Ouagadougou, Burkina Faso. *International Journal of Climatology*, 31:605–620. doi:10.1002/joc.2069

Majumdar S.J., and Coauthors (2020) Multiscale Forecasting of High-Impact Weather: Current Status and Future Challenges. *Bull. Amer. Meteor. Soc.,* doi: https://doi.org/10.1175/BAMS-D-20-0111.1.

Matthews, T.K.R., Wilby R.L., Murphy C. (2017) Global warming and deadly heat. *Proceedings of the National Academy of Sciences*, 114 (15), 3861-3866. doi:10.1073/pnas.1617526114

Matthews, T., Wilby, R.L., Murphy, C (2019) An emerging tropical cyclone–deadly heat compound hazard. *Nat. Clim. Change,* 9, 602–606. https://doi.org/10.1038/s41558-019-0525-6

Mora, C., Dousset, B., Caldwell, I. et al. (2017) Global risk of deadly heat. *Nature Clim Change,* 7, 501–506. https://doi.org/10.1038/nclimate3322

Moron V., Oueslati B., Pohl B., Rome S., Janicot S. (2016) Trends of mean temperatures and warm extremes in northern tropical Africa (1961–2014) from observed and PPCA-reconstructed time series. *J. Geophys. Res.*, 121:5298–5319, doi:10.1002/2015JD024303

Moron V., Oueslati B., Pohl B., Janicot S. (2018) Daily weather types in February–June (1979–2016) and temperature variations in tropical North Africa. *Journal of Climate*, 57:1171–1195. https://doi.org/10.1175/JAMC-D-17-0105.1.

Moron V., Robertson A.W., Wang L. (2019) Chapter 3 - Weather Within Climate: Sub-seasonal Predictability of Tropical Daily Rainfall Characteristics. In A.W. Robertson and F. Vitart (Ed.), *Sub-Seasonal to Seasonal Prediction* (pp. 47-64). Elsevier. https://doi.org/10.1016/B978-0-12-811714-9.00003-6

Naughton M.P., Henderson A., Mirabelli M.C., Kaiser R., Wilhelm J.L., Kieszak S.M., Rubin C.H., McGeehin M.A. (2002) Heat-related mortality during a 1999 heat wave in Chicago¹. *American Journal of Preventive Medicine*, 22 (4):221-227. doi:10.1016/S0749-3797(02)00421-X

Ndossi M.I., Avdan U. (2016) Application of Open Source Coding Technologies in the Production of Land Surface Temperature (LST) Maps from Landsat: A PyQGIS Plugin. *Remote Sensing*, 8(5):413. https://doi.org/10.3390/rs8050413

Offerle B., Jonsson P., Eliasson I., Grimmond C.S.B. (2005) Urban Modification of the Surface Energy Balance in the West African Sahel: Ouagadougou, Burkina Faso. *Journal of Climate*, 18:3983–3995. doi:10.1175/JCLI3520.1

Oueslati B., Pohl B., Moron V., Rome S., Janicot S. (2017) Characterization of heat waves in the Sahel and associated physical mechanisms. *Journal of Climate*, 30, 3095–3115. doi:10.1175/JCLI-D-16-0432.1

Ringard J., Dieppois B., Rome S., Diedhiou A., Pellarin T., Konare A., Konaré A., Diawara A., Konaté D., Dje B.K., Katiellou G.L., Seidou Sanda I., Hassane B., Vischel T., Garuma G.F., Mengistu G., Camara M., Diongue A., Gaye A.T., Descroix L. (2016) The intensification of thermal extremes in West Africa. *Global and Planetary Change*, 139:66–77. doi:10.1016/j.gloplacha.2015.12.009

Rossier C., and Coauthors (2012) The Ouagadougou Health and Demographic Surveillance System. *International Journal of Epidemiology*, 41 (3):658-666 doi:10.1093/ije/dys090

Russo S. and Coauthors (2014) Magnitude of extreme heat waves in present climate and their projection in a warming world. *J. Geophys. Res. Atmospheres*, 119:12500–12512, doi:10.1002/2014JD022098.

Russo S., Marchese A.F., Sillmann J., Immé G. (2016) When will unusual heat waves become normal in a warming Africa? *Environmental Res. Letters*, 11. doi.10.1088/1748-9326/11/5/054016

Sambou M-J.G., Janicot S., Pohl B., Badiane D., Dieng A.L., Gaye A.T. (2020) Heat wave occurrences over Senegal during spring: Regionalization and synoptic patterns. *International Journal of Climatology*, 40:440-457. doi:10.1002/joc.6220

Sambou M-J.G., Pohl B., Janicot S., Famien A.M., Roucou P., Badiane D., Dieng A.L. Gaye A.T. (2021) Heat waves in spring from Senegal to Sahel: Evolution under climate change. *International Journal of Climatology*, **in press**. doi:10.1002/joc.7176

Scott A.A., Misiani H., Okoth J., Jordan A., Gohlke J., Ouma G., et al. (2017) Temperature and heat in informal settlements in Nairobi. *PLoS ONE*, 12(11): e0187300. doi:10.1371/journal. pone.0187300

Semenza J.C., Rubin C.H., Falter K.H., Selanikio J.D., Flanders W.D., Howe H.L., Wilhelm J.L. (1996) Heat-Related Deaths during the July 1995 Heat Wave in Chicago. *New England Journal of Medicine*, 335 (2):84-90. doi:10.1056/NEJM199607113350203

Sobrino J.A., Jimenez-Munoz J.C., Paolini L. (2004) Land surface temperature retrieval from landsat TM 5. *Remote Sensing of environment*, 90(4):434–440. https://doi.org/10.1016/j.rse.2004.02.003

Sobrino J.A., Jiménez-Muñoz J.C., Sòria G., Romaguera M., Guanter L., Moreno J., Plaza A., Martínez P. (2008) Land surface emissivity retrieval from different VNIR and TIR sensors. *IEEE Transactions on Geoscience and Remote Sensing*, 46(2):316–327. doi:10.1109/TGRS.2007.904834

Steadman R.G. (1979) The assessment of sultriness. Part I: A temperature-humidity index based on human physiology and clothing science. *J. Appl. Meteor*., 18:861–873, doi:10.1175/1520-0450(1979)018,0861:TAOSPI.2.0.CO;2.

Tham S., Thompson R., Landeg O., Murray K.A., Waite T. (2020) Indoor temperature and health: a global systematic review. *Public Health*, 179:9-17. doi:10.1016/j.puhe.2019.09.005

Tyubee B.T., Iorpev P.S., Oche C.Y. (2020) Assessment of perceived and observed occupants' thermal comfort in residential buildings in Agan, Makurdi, Northcentral Nigeria. *Urban Climate*, 33:100633. doi:10.1016/j.uclim.2020.100633

Uejio C.K., Wilhelmi O.V., Golden J.S., Mills D.M., Gulino S.P., Samenow J.P. (2011) Intra-urban societal vulnerability to extreme heat: The role of heat exposure and the built environment, socioeconomics, and neighborhood stability. *Health & Place*, 17(2):498-507. doi:10.1016/j.healthplace.2010.12.005

Vandentorren S., Bretin P., Zeghnoun A., Mandereau-Bruno L., Croisier A., Cochet C., Ribéron J., Siberan I., Declercq B., Ledrans M. (2006) August 2003 Heat Wave in France: Risk Factors for Death of Elderly People Living at Home. *European Journal of Public Health,* 16 (6):583-591. doi:10.1093/eurpub/ckl063

Von Seidlein L., and Coauthors (2017) Affordable house designs to improve health in rural Africa: a field study from northeastern Tanzania. *The Lancet Planetary Health*, 1(5), e188-e199. doi:10.1016/S2542-5196(17)30078-5.

Wienert U., Kuttler W. (2005). The dependence of the urban heat island intensity on latitude–a statistical approach. *Meteorologische Zeitschrift*, 14(5):677-686. doi:10.1127/0941-2948/2005/0069

WHO (2018) WHO Housing and Health Guidelines. World Health Organization, Geneva

Xu Z., Fitzgerald G., Guo Y., Jalaludin B., Tong S. (2016) Impact of heatwave on mortality under different heatwave definitions: A systematic review and meta-analysis. *Environment International*, 89-90:193-203. doi:10.1016/j.envint.2016.02.007